Error Reduction in Magnetoquasistatic Positioning using Orthogonal Emitter Measurements

Darmindra D. Arumugam, *Member, IEEE,* Joshua D. Griffin, *Member, IEEE,* Daniel D. Stancil, *Fellow, IEEE,* and David S. Ricketts, *Member, IEEE*

***Abstract*—Measurements of the emitted magnetoquasistatic fields generated by a vertical emitting loop and detected at the terminals of seven fixed vertical receiving loops, all located above earth, are used to solve for position and orientation of the emitter. The coupling between the mobile emitting and fixed receiving loops was measured over a 3×3 emitter grid spanning an 18×18 m area, and for azimuthal orientations between 0° and 330° at 30° increments. Inverting the theoretical coupling expressions for two-dimensional position and azimuthal orientation resulted in a mean position and orientation error of 0.62 m and 2.86°, respectively. Calculations including orthogonal emitter configurations resulted in a mean position and orientation error of 0.21 m and 1.12°, respectively, which represents a 66.1 % and 60.8 % reduction in error, respectively.**

***Index Terms*—Electromagnetic fields, magnetoquasistatics, radio position measurement, radio tracking.**

I. Introduction

RECENTLY, position or orientation measurements of an electrically-small current loop generating magnetoquasistatic fields has been demonstrated by detecting the fields at one or more receiving loops and by inverting the field expressions for position or orientation [1]–[4]. Key to the magnetoquasistatic technique was the use of complex image theory to account for secondary fields due to induced eddy-currents within the earth that occur due to the close proximity of the current loop to the earth [1]. Accurate positioning is obtained even when the line-of-sight (LoS) is blocked by large groups of people [5]. One-dimensional (1D) distance measurements using a single receiving loop have achieved a root-mean-squared (RMS) error of 0.12 m over distances of up to 34.2 m [1]. By measuring the emitted field using seven receivers located outside a two-dimensional (2D) measurement grid spanning a 27.43×27.43 m area, a mean 2D geometric position error of 1.08 m was recently demonstrated by using a fixed azimuthal orientation of the vertical emitting loop [3].

This letter presents measurement results for the two-dimensional position and azimuthal orientation of the emitter measured over a 3×3 emitter grid spanning an 18×18 m area, and for azimuthal orientations between 0° and 330°. In addition to position and azimuthal measurements using a single emitter, we present calculations that use orthogonal emitter measurements at each location and show that they significantly reduce both position and orientation errors.

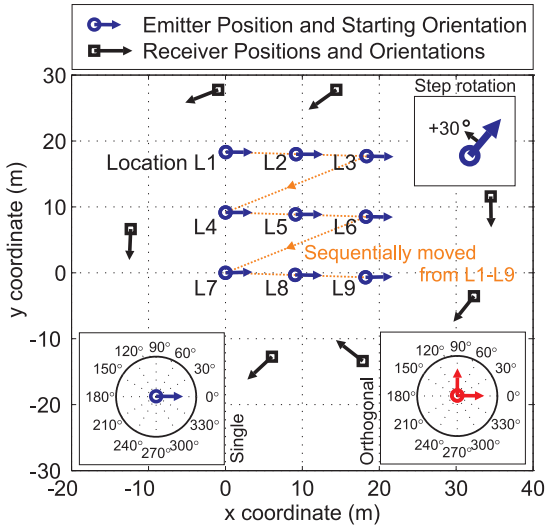

Fig. 1. The measurement grid obtained using the optical surveying instrument showing the actual position of the emitter at each location on the grid (L1-L9) and of the receivers outside the grid. The arrows on the emitter/receivers indicate the direction of the surface normal of the loop. The insets show the orientation of the single-emitter and orthogonal-emitter measurements and the 30° rotation of each. The orthogonal measurements are a superposition of two single antenna measurements, taken 90° apart from one another.

II. Complex Image and Positioning Theory

The magnetic field of a current loop in proximity to a conducting ground can be decomposed into the field of the loop and the induced eddy-currents in the ground [6]. Experiments have verified that complex image theory accurately models the secondary field due to the induced currents [1]. The total field outside the ground is given by:

$$H_p(x,y,z) = \vec{H}^d(x,y,z-h) + c_p\vec{H}^d(x,y,-z-\alpha), \quad (1)$$

where $p = ||, \perp$ describes fields parallel and perpendicular to the ground, $c_{||} = 1$ and $c_\perp = -1$, $\alpha = h + \delta(1-j)$, δ is the skin depth, and $\vec{H}^d$ is the dipole field given by [7]:

$$\vec{H}^d(x,y,z) = \frac{1}{4\pi}\left[\frac{3\vec{r}(\vec{m}\cdot\vec{r}) - \vec{m}r^2}{r^5}\right], \quad (2)$$

where $\vec{m}$ is the moment and $\vec{r}$ is the position vector from the origin to observation. The theoretical description of the voltage

D. D. Arumugam was with the Department of Electrical and Computer Engineering, Carnegie Mellon University, Pittsburgh, PA, 15213. He is currently with Jet Propulsion Laboratory, California Institute of Technology, Pasadena, CA, 91109 USA e-mail: darmindra.d.arumugam@jpl.nasa.gov.

J. D. Griffin is with Disney Research Pittsburgh, Pittsburgh, PA, 15213 USA e-mail: joshdgriffin@disneyresearch.com.

D. D. Stancil is with the Department of Electrical and Computer Engineering, North Carolina State University, Raleigh, NC, 27695 USA e-mail: ddstancil@ncsu.edu.

D. S. Ricketts is with the Department of Electrical and Computer Engineering, Carnegie Mellon University, Pittsburgh, PA, 15213 USA e-mail: ricketts@ece.cmu.edu.

at the terminals of any receiver shown in Fig. 1 is given by:

$$V^T = -j\omega\mu_o \left[\hat{n} \cdot \left(\vec{H}_{||} + \vec{H}_{\perp}\right)\right] a, \tag{3}$$

where $\hat{n}$ is the unit vector normal to the receive loop and a is the surface area of the loop. Use of k fixed receivers with known positions and orientations, as shown in Fig. 1 for $k = 7$, generates a set of k equations from which the emitter's unknown position and orientation can be found. This is done by minimizing the sum of squared difference between the measured voltage (V^M) at the terminal of each loop and the expression in (3):

$$\Phi = \sum_{i=1}^{k} \left[V_i^T - V_i^M\right]^2, \tag{4}$$

using a numerical, nonlinear, least-square optimization algorithm. We employ a trust-region reflective optimization algorithm [8]. This algorithm generates lower-dimensional trust-regions, within which trial steps are used to force global convergence via the steepest descent direction. Local convergence is found using the Newton step. The algorithm is effective on sparse problems.

III. Description of Experiment

The purpose of the present experiment is to study the error in the 2D magnetoquasistatic position measurements, as described in [3], over a measurement grid for variations in azimuthal orientation of the emitter. Because the coupling between the emitter and each fixed receiver (2)-(3) is a function of the emitter azimuthal orientation, we expect the error to vary as a function of orientation. Further, because the solution for position is found by minimizing the sum of squared difference in the equations in (4), where each equation describes the coupling between the emitter and individual receiver, we expect higher errors to arise in configurations where the dipole field of the emitter is at a null with one or more receivers.

One approach to solving this problem is to use orthogonal emitting loops (two co-located vertical loops with azimuthal orientation separation of 90°), which provide strong coupling from one loop when the other emitting loop is weakly coupled due to a null dipole field. Orthogonal loops have been used in the past for orientation tracking [9], for underground direction finding [10], and more recently for short range position and orientation tracking [11], [12]. In each case, the orthogonal loops are used to provide adequate number of unique equations, i.e., additional measurements, to provide a unique solution to orientation, direction, or position and orientation. To the best of our knowledge, orthogonal loops have not been used in the manner discussed in this paper, where orthogonal measurements are conducted to eliminate weak coupled fields and provide a reduced set of equations which consistently provide strong coupling, i.e., good SNR.

Additional co-located vertical loops at different azimuthal orientations, beyond two orthogonal vertical loops, will provide incremental reduction in the positioning error when the emitter's orientation is such that the additional antennas provide stronger coupling with the receivers than the two orthogonal loops. Since some mobile applications may have weight constraints, we haven chosen to study only the two orthogonal loop case to minimize the number of antennas on the emitter. Additional non-vertical loops would aid significantly in out-of-plane measurement, e.g., three-dimensional measurements, and especially when the inclination orientation of the source is varied.

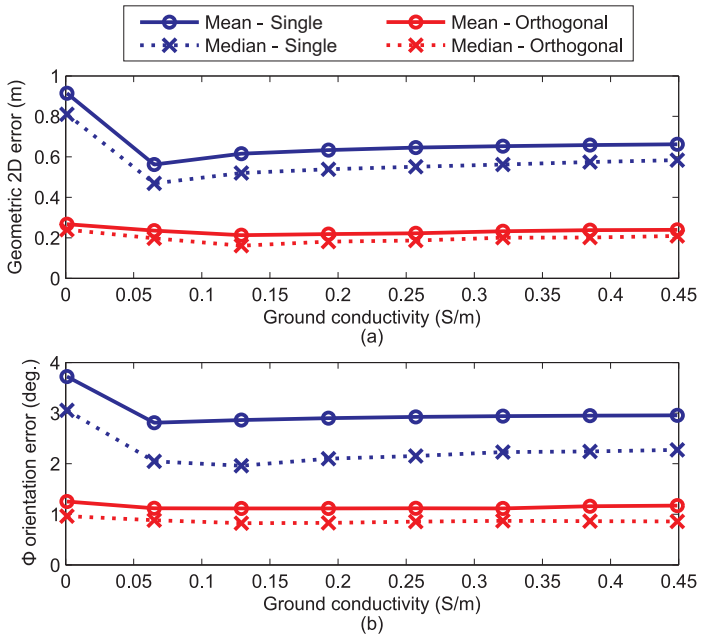

Fig. 2. Measurements of geometric position error (a) and orientation error (b) for both the single-loop and orthogonal-loops configurations, and for ground conductivity values between 0.001 S/m and 0.5 S/m. The minimum error is achieved with a ground conductivity of 0.065 S/m.

Our purpose here is to study the use of two orthogonal vertical loops in reducing the positioning errors. We can investigate the efficacy of such orthogonal loops by using measurements from a single emitting loop, taken at two azimuthal angles 90° apart (see inset of Fig. 1). Using this technique, we only require a single emitter to study the orthogonal measurement result, thus the measurements for the orthogonal configurations are taken with exactly the same hardware. The emitter used for this purpose is composed of a 50-turn coil [34 American Wire Gauge (AWG) wire] driven by a class-E oscillator circuit, with power supplied through a 9V battery [3]. The loop is coiled around a hollow dielectric [Delryn/Acetal (polyoxymethylene)] tube with an outer diameter of 16.5 cm. The setup is also held on a dielectric tripod and the loop is elevated to a height of 0.6 m above the ground. The class-E oscillator circuit driving the emitting loop generates a signal at 360 kHz with an output power of 0.56 W at an efficiency of 93%. Each of the seven receivers denoted in Fig. 1 is composed of an active receiving loop with a diameter of 1 m (LFL-1010 by Wellbrook Communications), a band-pass filter to attenuate unwanted signals (band-pass region of 300-450 kHz), and a low-noise amplifier (AD8331 by Analog Devices) [3]. The resulting signal at the terminals of the amplifier is digitized using a 16-bit 10 MS/s analog-to-digital converter (ADC) included in the PXI-9816D/512 digitizer by Adlink Technologies, from which a Fast-Fourier Transform algorithm is used to convert the time-domain sig-

nals to frequency-domain. The peak signal at approximately 360 kHz is used to determine the measured voltage, V^M, at each receiver in (4).

The measurement grid obtained using measurements with optical surveying instrumentation and reflectors (see [3], Fig. 5), and used for the two-dimensional position and azimuthal orientation experiment is shown in Fig. 1. The emitter is positioned sequentially through a 3×3 grid spanning an 18×18 m area from location L1 through L9, and seven receivers are located outside the measurement grid. At each location of the emitter, the azimuthal orientation of the emitter is varied between 0° and 330° in 30° increments, as indicated in the inset in Fig. 1 where the arrows indicate the direction of the surface normal of the loops. The measurement setup for the emitter system as well as each receiver system are identical to those described in [3]. The grid measurements were also conducted on the same outdoor grass-field (see [3], background of Fig. 5). The optical surveying instrument was used to obtain the position and orientation of each receiving loop, which was then used to reduce the theoretical expression describing the coupling (2)-(3) to have a total of six unknowns, the x, y, and z position and θ and ϕ orientation of the emitter, and the ground conductivity (σ) of the earth. At each measurement position and orientation, optical measurements of the emitter were also conducted, and by using optically measured values for z and θ, the six unknowns are reduced to four, the x and y position and ϕ orientation of the emitter, and the ground conductivity, σ.

By minimizing the sum of squared difference between the measured voltage and theoretical description of the reduced set of seven equations, describing the coupling between each receiver and the emitter, we find the x and y position and ϕ orientation of the emitter at each measurement position and orientation for a given value of ground conductivity. Figure 2 is a plot of the mean and median geometric position error (a) and orientation error (b) for ground conductivity values between 0.001 S/m and 0.5 S/m. The *single emitter* results indicate azimuthal variations of the emitter between 0° and

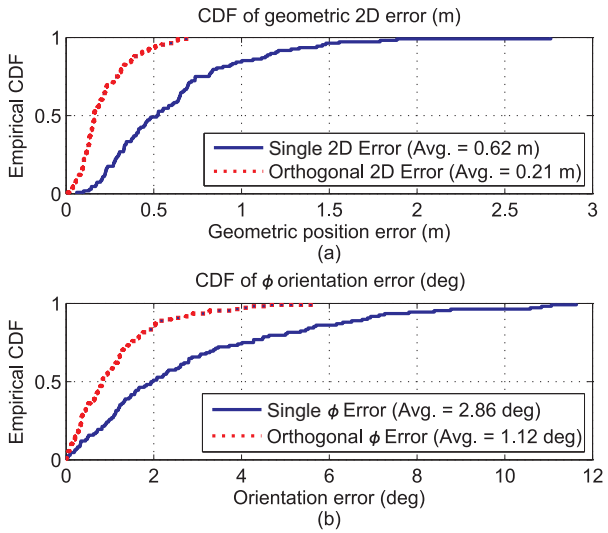

Fig. 3. Cumulative distribution of measurement results for geometric position error (a) and orientation error (b) for both the single-loop and orthogonal-loop configurations, and for a ground conductivity of 0.065 S/m.

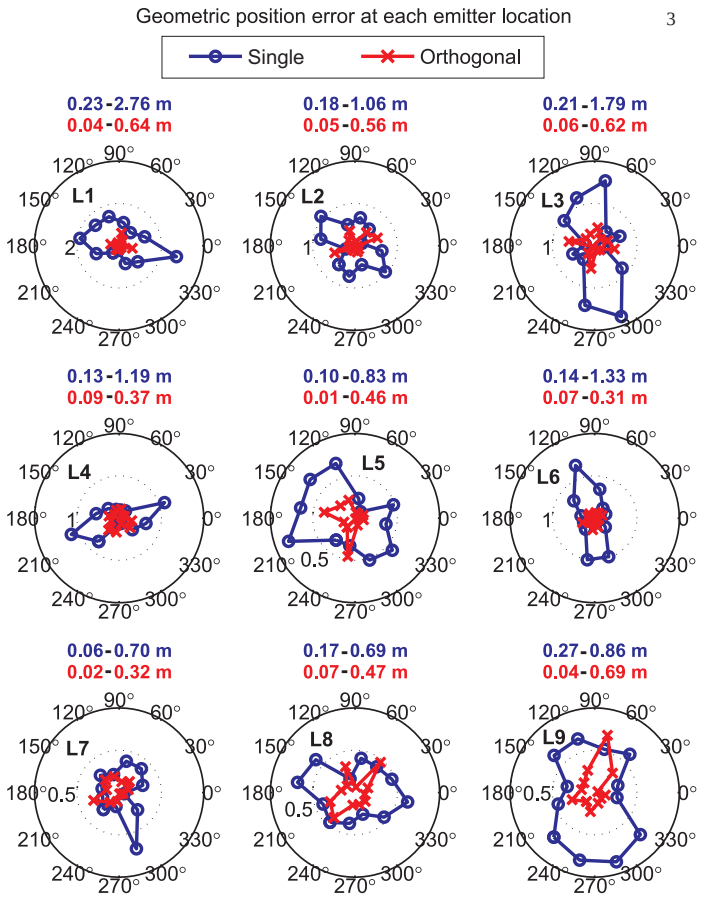

Fig. 4. Geometric position error at each emitter location (L1-L9) on the measurement grid for variation in azimuthal orientation of the emitter, and for both the single emitter and orthogonal loop configuration. Minimum and maximum position errors are shown above each plot, with the single emitter configuration listed on top.

330° at 30° increments. The *orthogonal* results indicate the use of orthogonal emitter measurements to solve for position and orientation. For example, at each location on the grid (L1-L9), we have azimuthal orientation measurements at ϕ = [0,30,60,$\cdots$ 330]°. For the *orthogonal* results, we use ϕ = 0° and 90° for the first set of orthogonal emitter measurements, then ϕ = 30° and 120°, then ϕ = 60° and 150°, and so on. By using the *orthogonal* configuration, the total number of equations that describe the coupling between the emitter and all receivers is doubled from seven to fourteen. However, at each instance we compare the two measurements of the *orthogonal* configuration and retain only the larger measured value, which reduces the total equations to seven and eliminates the weak coupling associated with nulls of the emitted field. In total, there are an equal number of 12[1] *single emitter* and *orthogonal* results at each location shown in Fig. 1. The result shows a minimum mean and median error for the *single* emitter configuration at a ground conductivity of σ = 0.065 S/m. The mean and median results for the *orthogonal* emitter configuration are noticeably reduced when compared to the *single* emitter configuration for all values of ground conductivity. The reduced geometric error curves for

[1]The single emitting loop configuration is rotated in steps of 30° at each location L1-L9. This corresponds to 12 measurements at each location or a total of 108 measurements in the entire grid. At each location, the 12 measurements can be used to process 12 single emitter configurations or 12 orthogonal emitter configurations. The 12 orthogonal emitter configurations are obtained by using single emitter configurations which are 90° apart.

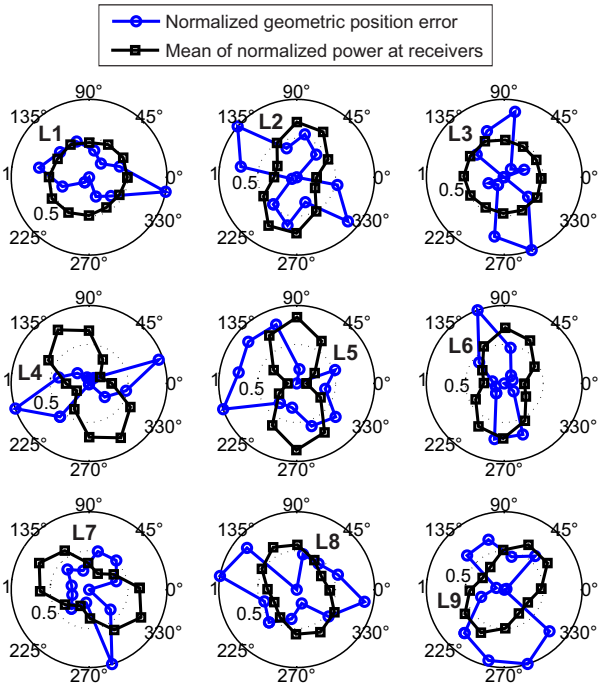

Fig. 5. The mean of normalized power measured at all receivers, analyzed alongside the normalized single emitter geometric position error for all emitter locations L1-L9.

the orthogonal measurement results are less sensitive to ground conductivity than the single emitter measurements. This is largely due to the fact that for geometric distances used in the measurements between the receivers and the emitter locations, the 1D RMS error is on the order of 0.12 m [1], and thus we expect a lower bound 2D geometric position error on the order of $\left[0.12^2 + 0.12^2\right]^{1/2} = 2^{1/2} \times 0.12$ m=0.17 m which would saturate the curve to a minimum value of this order.

Using a ground conductivity value of 0.065 S/m, a cumulative distribution function (CDF) is plotted in Fig. 3 for the measured two-dimensional geometric (a) and azimuthal orientation (b) errors. The results show a significant reduction in cumulative errors when using the *orthogonal* emitter configurations. The median *orthogonal* geometric and orientation error is 0.16 m and 0.82°, respectively, compared to 0.52 m and 1.96° for the *single emitter* configuration. Similarly, the mean *orthogonal* geometric and orientation error is found to be 0.21 m and 1.12°, respectively, compared to 0.62 m and 2.86° for the *single emitter* configuration. This corresponds to a 66.1 % and 60.8 % reduction in the mean two-dimensional geometric and azimuthal orientation error, respectively.

Figure 4 shows the error measured at each increment of azimuthal orientation and at each location (L1-L9) on the two-dimensional grid. In almost all cases, the *single emitter* position error shows two lobes corresponding to higher position errors. These large, approximately-symmetric error lobes are not present in the *orthogonal* configurations, which suggest that they are potentially caused by symmetric dipole field coupling nulls, where the position estimation is expected to incur a larger error due to low signal power, i.e., low SNR.

To study the emitter-receiver field coupling nulls, Fig. 5 presents the analysis of the mean normalized power measured at all receivers overlaid with the normalized single emitter geometric position error for all emitter locations L1-L9. We normalize each receiver's signal power to its maximum to illustrate the spatial distribution, i.e., location of the nulls. If we had normalized to the maximum or average power of all signals, we would not see the spatial distribution of each received signal as clearly. Emitter locations L1 and L3 show a mean of normalized power curve that has a circular pattern, suggesting that the nulls (or broadside) of the field couplings measured at all receivers are evenly spread throughout all orientations. For these locations, it is difficult to assert (although it cannot be ruled out) that higher position errors are due to nulls in the measured field couplings. Out of the remaining locations, all except for emitter location L6 show increased single emitter geometric position error in orientations where nulls in the field couplings are generally clustered. Note however that the approximately-symmetric lobes of the single emitter position errors and the mean of received power are not always completely orthogonal to each other, which warrants a more detailed future study.

IV. Conclusions

We extended our 2D magnetoquasistatic position measurements in [3] to include the effects of azimuthal orientation variation at each location on the measurement grid and demonstrated a significant reduction in position and orientation error by using orthogonal configurations of the emitter. Use of the orthogonal emitter configuration resulted in a mean position and orientation error of 0.21 m and 1.12°, respectively, which represents a 66.1 % and 60.8 % reduction in error, respectively, when compared to the single emitter configuration.

References

[1] D. Arumugam, J. Griffin, and D. Stancil, "Experimental Demonstration of Complex Image Theory and Application to Position Measurement," *IEEE Antennas Wireless Propag. Lett.*, vol. 10, pp. 282–285, April 2011.

[2] D. Arumugam, J. Griffin, D. Stancil, and D. Ricketts, "Higher Order Loop Corrections for Short Range Magnetoquasistatic Position Tracking," in *IEEE International Symp. on Antennas and Propag*, July 2011, pp. 1755–1757.

[3] ——, "Two-dimensional position measurement using magnetoquasistatic fields," *Antennas and Propagation in Wireless Communications (APWC), 2011 IEEE-APS Topical Conference on*, pp. 1193–1196, Sept. 2011.

[4] ——, "Wireless orientation sensing using magnetoquasistatic fields and complex image theory," *Radio and Wireless Symposium (RWS), 2012 IEEE*, pp. 251–254, Jan. 2012.

[5] ——, "Experimental study on the effects of groups of people on magnetoquasistatic positioning accuracy," *IEEE International Symp. on Antennas and Propag,*, 2012, accepted.

[6] J. Weaver, "Image approximation for an arbitrary quasi-static field in the presence of a conducting half space," *Radio Science*, vol. 6, no. 6, pp. 647–653, June 1971.

[7] J. Jackson, "Classical Electrodynamics," John Wiley and Sons Inc., 1999.

[8] T. Coleman and Y. Li, "An interior trust region approach for nonlinear minimization subject to bounds," *SIAM Journal on Optimization*, vol. 6, no. 2, pp. 418–445, 1996.

[9] H. P. Kalmus, "A new guiding and tracking system," *Aerospace and Navigational Electronics, IRE Transactions on*, vol. ANE-9, no. 1, pp. 7 –10, march 1962.

[10] R. Olsen and A. Farstad, "Electromagnetic direction finding experiments for location of trapped miners," *Geoscience Electronics, IEEE Transactions on*, vol. 11, no. 4, pp. 178 –185, oct. 1973.

[11] F. Raab, "Quasi-static magnetic-field technique for determining position and orientation," *IEEE Trans. on Geoscience and Remote Sensing*, vol. GE-19, no. 4, pp. 235–243, October 1981.

[12] F. Raab, E. Blood, S. T., and J. H., "Magnetic Position and Orientation Tracking System," *IEEE Trans. on Aerospace and Electrical Systems*, vol. AES-15, no. 5, pp. 709–718, 1979.